



## Temperature-Aware gm/ID-based Methodology for Active Inductor Design

João R. Raposo de O. Martins, Emilie Avignon-Meseldzija, Pietro Maris Ferreira

### ► To cite this version:

João R. Raposo de O. Martins, Emilie Avignon-Meseldzija, Pietro Maris Ferreira. Temperature-Aware gm/ID-based Methodology for Active Inductor Design. Workshop on Circuits and System Design, Aug 2019, São Paulo, Brazil. hal-02268794

**HAL Id: hal-02268794**

**<https://centralesupelec.hal.science/hal-02268794>**

Submitted on 23 Sep 2019

**HAL** is a multi-disciplinary open access archive for the deposit and dissemination of scientific research documents, whether they are published or not. The documents may come from teaching and research institutions in France or abroad, or from public or private research centers.

L'archive ouverte pluridisciplinaire **HAL**, est destinée au dépôt et à la diffusion de documents scientifiques de niveau recherche, publiés ou non, émanant des établissements d'enseignement et de recherche français ou étrangers, des laboratoires publics ou privés.

# Temperature-Aware gm/ID-based Methodology for Active Inductor Design

João R. Raposo de O. Martins, Emilie Avignon-Meseldzija, Pietro Maris Ferreira

## ► To cite this version:

João R. Raposo de O. Martins, Emilie Avignon-Meseldzija, Pietro Maris Ferreira. Temperature-Aware gm/ID-based Methodology for Active Inductor Design. Workshop on Circuits and System Design, Aug 2019, São Paulo, Brazil. hal-02268794

**HAL Id: hal-02268794**

**<https://hal-centralesupelec.archives-ouvertes.fr/hal-02268794>**

Submitted on 23 Sep 2019

**HAL** is a multi-disciplinary open access archive for the deposit and dissemination of scientific research documents, whether they are published or not. The documents may come from teaching and research institutions in France or abroad, or from public or private research centers.

L'archive ouverte pluridisciplinaire **HAL**, est destinée au dépôt et à la diffusion de documents scientifiques de niveau recherche, publiés ou non, émanant des établissements d'enseignement et de recherche français ou étrangers, des laboratoires publics ou privés.

# Temperature-Aware gm/ID-based Methodology for Active Inductor Design

João R. Raposo de O. Martins, Emilie Avignon-Meseldzija, Pietro M. Ferreira

[joao-roberto.raposo,emilie.avignon]@centralesupelec.fr,maris@ieee.org

GeePs, UMR CNRS 8507, CentraleSupélec, Univ. Paris-Sud, Université Paris-Saclay, Gif-sur-Yvette, France

## ABSTRACT

Active inductors have become standard building blocks for many applications by its reconfigurability and reduced silicon area. However, the inductance variation over temperature is a main circuits' limitation in harsh environments. This paper presents a novel temperature analysis of a general architecture of active inductors, obtaining an optimal conductance value to minimize inductance variation over temperature. Based on the  $g_m/I_D$  and sensitivity analysis, temperature variation result highlights that, even if its counter intuitive to bias transistors in weak inversion, a low inductance variation of 139 ppm/°C is obtained from -45 to 175 °C.

## CCS CONCEPTS

• Hardware → Analog and mixed-signal circuit synthesis.

## KEYWORDS

temperature-aware, gm/ID methodology, active inductors, harsh environment

## ACM Reference Format:

João R. Raposo de O. Martins, Emilie Avignon-Meseldzija, Pietro M. Ferreira. 2019. Temperature-Aware gm/ID-based Methodology for Active Inductor Design. In *9th Workshop on Circuits and System Design (WCAS '19)*, August 26–30, 2019, Sao Paulo, Brazil. ACM, New York, NY, USA, 4 pages. <https://doi.org/>

## 1 INTRODUCTION

Internet of Things has brought the need for novel studies in order to address communication devices requirements, driven specifically by the Smart Vehicle industry [5]. In smart vehicles applications, the circuit specification is strictly regulated by security and safety standards. Reliability and robustness in the device operation must be ensured for harsh environments, including the required operating temperature range from -40 to 175 °C.

Receivers and transmitters nowadays are mainly dedicated to the digital signal processing. In this context, the analog front-end is only reserved to the signal conditioning before the analog-to-digital conversion or to the amplification before transmission. In such devices, the use of inductors is indispensable for impedance matching [11] or bandwidth extension [4]. The need for a large

silicon area to fabricate spiral inductors and transformers has also sparked a great interest in and an intensive research on the synthesis of inductors and transformers using active devices [15].

Active inductors (AI) have noticeable advantages as: low surface, reconfigurability, and digital CMOS compatibility. However, AI's major drawbacks are poor noise performance and power consumption. J. Ou and P.M. Ferreira have analyzed the power consumption and noise of those devices [10]. Design considerations are revealed in order to optimize AIs. However, the temperature dependency is indicated in [1] as a major challenge for AIs design. V. Kulmar *et al.* have presented new results of temperature variation effects in different AIs topologies [8]. Temperature-analyses of the variation of central frequency of a LC oscillator is revealed, and a best-case scenario is shown for a resonant frequency variation of 4.6 GHz from -20 °C to 100 °C.

Still, no design methodology is available to minimize performance variation over temperature. This paper presents an analysis of the overall thermal stability of a generic AI to propose a  $g_m/I_D$ -based design methodology. The proposal is exemplified by an AI design using XFAB 0.18  $\mu\text{m}$  technology. Post-layout results are presented to validate the proposal from -40 to 175 °C.

## 2 ACTIVE INDUCTOR

Active inductor implementations usually come from gyrators theory, and can be implemented by connecting two transconductors back-to-back as shown in Fig. 1.

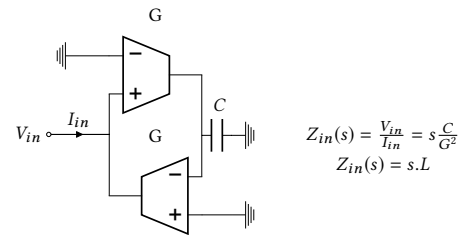


Figure 1: A Gyrator-C model representation

In order to evaluate the temperature variation effects, the transconductance is assumed to be the only temperature dependent value since  $C$  is determined by physical dimensions and properties of the device, leading to

$$L(T) = \frac{C}{G_1(T) G_2(T)}. \quad (1)$$

A sensitivity function ( $S_x^{f(x)}$ ) is defined as the percentage variation of  $f(x)$  as  $x$  varies 1%, mathematically expressed as

$$S_x^{f(x)} = \frac{\frac{\Delta f(x)}{f(x)}}{\frac{\Delta x}{x}} \approx \frac{x}{f(x)} \cdot \frac{df(x)}{dx}. \quad (2)$$

Calculating the inductance value  $L(T)$  sensitivity to temperature, one may find

$$\begin{aligned} S_T^{L(T)} &= \frac{T}{L(T)} \cdot \frac{dL(T)}{dT} \\ &= -T \left( \frac{1}{G_1} \frac{dG_1(T)}{dT} - \frac{1}{G_2} \frac{dG_2(T)}{dT} \right) \end{aligned} \quad (3)$$

To minimize the temperature effects on the inductance value and consequently  $S_T^{L(T)}$ , an optimal  $G(T)$  behavior should be found, thus

$$\begin{aligned} C[G(T)_{1,2}] &= \langle S_T^{L(T)}; S_T^{L(T)} \rangle = \int_0^\infty \left( S_T^{L(T)} \right)^2 dT \\ &= \int_0^\infty \frac{T^2 (G_2(T)G_1'(T) + G_1(T)G_2'(T))^2}{G_1(T)^2 G_2(T)^2} dT. \end{aligned} \quad (4)$$

This minimization problem can be solved by a calculus of variations method and the solution is given by solving the Euler-Lagrange system equations:

$$\begin{aligned} \nabla C[G_{1,2}(T)] &= \frac{\partial L}{\partial G_{1,2}}(T, G_{1,2}, H_{1,2}) \\ &\quad - \frac{d}{dx} \left( \frac{\partial L}{\partial H_{1,2}}(T, G_{1,2}, H_{1,2}) \right) = 0 \\ L[T, G_{1,2}, H_{1,2}] &= \frac{T^2 (G_2(T)H_1(T) + G_1(T)H_2(T))^2}{G_1(T)^2 G_2(T)^2} \\ H_{1,2} &= \left( \frac{dG_{1,2}(T)}{dT} \right), \end{aligned} \quad (5)$$

applying the boundary condition that  $G_0 = G(T_0)$  and solving (5) the optimal found is

$$G_{1,2}(T) = G_0 \cdot e^{\pm \alpha(T-T_0)}. \quad (6)$$

This solution can be proved by using the theorem described in [7].

### 3 TEMPERATURE EFFECTS ON CMOS TRANSISTORS

Actual AI implementations typically uses MOSFETS gyrators, those transistor models are usually derived from two limit situations in [6]. The first one, weak inversion (WI), is obtained when the gate to source voltage ( $V_{GS}$ ) is lower than the threshold voltage ( $V_{th}$ ). Otherwise when  $V_{GS} \gg V_{th}$ , it is said that the transistor works in strong inversion (SI) regime. Transistor IxV characteristics are described in [2] and in [6] as

$$\begin{aligned} I_D \Big|_{WI} &= I_0 \cdot \frac{W}{L} e^{\frac{V_{GS}-V_{th}}{n\phi_t}} \cdot (1 - e^{-\frac{V_{DS}}{\phi_t}}), \\ I_D \Big|_{SI} &= \frac{\mu \cdot C_{ox}}{2} \cdot \frac{W}{L} \cdot (V_{GS} - V_{th})^2. \end{aligned} \quad (7)$$

The  $C_{ox}$  is the gate oxide capacitance density;  $\frac{W}{L}$  is the transistor aspect ratio;  $\mu$  is the carriers mobility; The  $\phi_t$  is the thermal voltage defined as  $\frac{k \cdot T}{q}$ , where  $k$  is the Boltzmann constant,  $q$  the electron

charge and  $T$  the absolute temperature in Kelvin. It is important to point out that, in [2], the  $I_0$  temperature dependency is not explicit, however it can be shown that it is proportional to  $C_{ox} \cdot \mu \cdot \phi_t^2$  [9]. The body and Drain-induced barrier lowering (DIBL) effects were omitted on (7) for reader clarity.

To fully analyze the transistor performance in temperature, one need to model their parameters behavior defined as

$$\begin{aligned} V_{th}(T) &= V_{th0} \cdot [1 + \alpha_{th}(T - T_0)], \\ \mu(T) &= \mu_0 \left( \frac{T}{T_0} \right)^{-\alpha_\mu}, \end{aligned} \quad (8)$$

where based on the Boltzmann Transport Equation solution,  $\alpha_\mu$  is bias dependent. That can be explained by the fact that when electric field is low (i.e. WI), the transport phenomena is dominated by the diffusion effect having a positive temperature dependency due to thermal excitation [9]. Considering the increase in the channel electric field and subsequently the  $V_{GS}$ , the drift effect is predominant given a negative temperature dependency to the current density due to the energy losses by phonon emission. On both regions, one can define the small signal drain to source conductance ( $g_{ds}$ ) and gate voltage to drain current transconductance ( $g_m$ ) by following [6] model.

#### 3.1 Temperature-aware sensitivity analysis

Model in [6] allows the definition of analytical expression for the different  $g_m/I_D$  temperature sensibilities on both WI and SI. The  $\lambda$  is the DIBL factor, which is described in [13] as temperature invariant. Those expressions can be useful when analyzing the sensitivity in a circuit where the transistors bias is known.

$$\begin{aligned} S_T^{J_{DS}} \Big|_{WI} &= 2 - \alpha_\mu \frac{V_{GS}}{\phi_t}, \\ S_T^{J_{DS}} \Big|_{SI} &= -2 \frac{\alpha_{th} \cdot T \cdot V_{th0} + \alpha_\mu (V_{GS} - V_{th}(T))}{V_{GS} - V_{th}(T)}, \\ S_T^{g_m} \Big|_{WI} &= -\frac{1}{\phi_t} \frac{V_{DS} \operatorname{csch}(V_{DS}/(2\phi_t))}{4 \cdot \lambda - 2 \cdot n(1 + \tanh(V_{DS}/(2\phi_t)))}, \\ S_T^{g_{ds}} \Big|_{SI} &= S_T^{J_{DS}} \Big|_{SI}, \\ S_T^{g_m} \Big|_{WI} &= -1, \\ S_T^{g_m} \Big|_{SI} &= \frac{2\alpha_{th}}{(V_{GS} - V_{th}(T))^2}. \end{aligned} \quad (9)$$

### 4 AI DESIGN EXAMPLE

In order to validate the hypothesis made in Sections 2 and 3, a transistor-level AI is designed. Figure 2(a) illustrates the chosen AI topology. Figure 2(b) is the AI model used in this work. In Fig. 2(a), the  $M_p$  transistor works as a transconductance in SI, and the  $M_n$  transistor works as a simple voltage-controlled resistor. So the conductance required in (1) are  $g_{mp}$  and  $g_{dsn}$ . If  $M_n$  is biased in WI it  $g_{ds}$  presents a high exponential temperature characteristic, as desired in(6). Since  $V_{DS}$  is too small, one can write

$$g_{ds} \Big|_{WI} = \frac{\phi_t^3}{2} \cdot C_{ox} \cdot \mu(T) \cdot \frac{W}{L} \cdot n \cdot e^{\frac{V_{GS}-V_{th}}{n\phi_t}}. \quad (10)$$

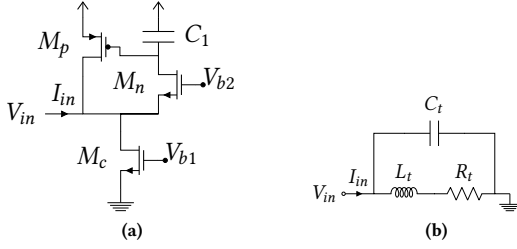


**Figure 2: (a) AI implementation proposed in [10] and (b) the transistor level model from [15]**

In addition,  $\phi_t$  is in the order of tenths of millivolts, and thus  $\phi_t^3$  can be considered negligible. The equivalent model values are calculated as:

$$\begin{cases} L_t = \frac{C_1}{g_{dsn}(g_{dsp} + g_{mp})}, \\ R_t = \frac{1}{g_{dsp} + g_{mp}}, \\ C_t = C_{gsn} + C_{gdc} + C_1 + \frac{C_1 \cdot g_{dsp}}{g_{dsn}}. \end{cases} \quad (11)$$

The  $M_p$  drain to source conductance appears as a parasitic effect due to the DIBL and can be minimized by using large length transistors. In order to analyze the different parameters contribution to the overall temperature sensitivity using the  $g_m/I_D$  methodology, one can find  $L_t$  as

$$L_t = \frac{1}{W_t \cdot J_{DSn} \cdot J_{DSP}} \cdot \frac{C_1 \cdot g_{mn} / g_{dsn}}{(g_{dsp} / I_{Dp} + g_m / I_{Dp}) \cdot g_m / I_{Dn}}, \quad (12)$$

where  $W_t = W_p \cdot W_n$ . Since wide channel transistors are used, one may assume  $g_{dsp} / I_{Dp} \ll g_m / I_{Dp}$ . Using this approximation, one may calculate the overall inductance sensitivity to the temperature as

$$S_T^{L_t} \approx S_T^{\frac{g_m}{g_{dsn}}} - (S_T^{\frac{g_{mn}}{I_{Dn}}} + S_T^{J_{dsp}} + S_T^{J_{dsn}} + S_T^{\frac{g_{mp}}{I_{Dp}}}). \quad (13)$$

As a consequence of no DC path on  $M_n$   $I_{Dn}$ , one can suppose that its drain to source voltage is very low, making this approximation in the equations deduced in Sec. 3 and considering WI the following approximation is valid:

$$S_T^{\frac{g_m}{g_{dsn}}} = S_T^{\frac{g_{mn}}{I_{Dn}}} = -1. \quad (14)$$

Therefore, it is possible to nil  $S_T^{L_t}$  by making

$$S_T^{J_{DSn}} + S_T^{J_{DSP}} + S_T^{g_{mp}/I_{Dp}} = 0. \quad (15)$$

#### 4.1 Temperature-aware transistor analysis

The XH018 process technology from the XFAB Silicon Foundries is chose in this work. XH018 technology is ideal for system-on-chip (SoC) applications in the automotive market such as high-voltage control devices, in engine compartments or housings circuitry with temperature range up to 175 °C, as well as embedded low-voltage applications in the communications, consumer and industrial market [14].

In order to evaluate the different sensibilities on the XH018, parameters were estimated (electrical simulation) by injecting a desired drain to source current over a normalized MOSFET with a

width of 1  $\mu\text{m}$  using an ideal Wilson's current mirror. The simulated sensibilities are shown in Fig. 3(a), 3(b) and 3(c).

With the different sensibilities calculated it is possible to numerically determinate the optimal  $J_{DS}^*$  by finding the values that nil (15). Analytical results are depicted in dashed blue line in Fig. 4. It presents a strong exponential characteristic in agreement to simulation data in continuous red line, which validates the proposal in Sec. 2. Thus, a fitting was carried out in  $J_{DS}$  expression to obtain

$$g_{mp}^* = \frac{2 \cdot J_{DS}^* \cdot W}{(V_{GS} - V_{th})} = G_0 \cdot e^{C_1(\frac{1}{T_0} - \frac{1}{T})}. \quad (16)$$

Since  $V_{GS}$  is fixed by the circuit,  $V_{th}$  presents a linear dependency on temperature as

$$J_{DS}^* = G_0 \cdot e^{\alpha(T-T_0)} (V_{GS} - V_{th0}(1 + \alpha_{th}(T - T_0))). \quad (17)$$

To achieve this result a beta multiplier reference [3] using a negative temperature coefficient was designed using Spectre Virtuoso global optimization tools. Temperature characteristics match the second order Taylor series of (17). The  $M_c$  and  $M_p$  transistor width was chosen in order to have to desired  $J_{DS}^*$  of 400  $\mu\text{A}/\mu\text{m}$  at 27 °C, their lengths where chosen to bias the transistor in SI with  $I_{DS} \leq 500 \mu\text{A}$ . The final values obtained are:  $W_p = W_2 = 1.6 \mu\text{m}$ ,  $W_n = 880 \text{ nm}$ ,  $W_1 = 2 \mu\text{m}$ ,  $L = 680 \text{ nm}$ ,  $k = 0.25$ ,  $R = 1.47 \text{ k}\Omega$ .  $W_1$  are the PMOS transistor widths of the beta multiplier,  $W_2$  the NMOS beta multiplier width and  $k$  the ration between the beta multiplier's NMOS width.

#### 4.2 Post-Layout Simulation Results

The AI layout was implemented using Cadence Virtuoso with the XTH018 design kit having an area of 15.6 x 10.4  $\mu\text{m}^2$ , circuit layout was omitted due to the lack of space. Post-layout 80-points Monte Carlo S-parameters (from  $V_{in}$  to  $V_{b2}$  ports) simulations are carried out for 221-points temperature variation from -40 to 175 °C. The input impedance is obtained from the  $V_{in}$  node and the inductance value is extracted.

Figure 5(a) compares the optimized active inductor design, in blue, using the sensitivity analysis with a reference active inductor design, in orange, with a simple current mirror bias. Only mean results of Monte Carlo simulation are presented; they are normalized for  $L_t = 2.65 \mu\text{H}$ . Optimized inductor presents a variation below 3 %, while reference design varies for 100 % for a temperature variation from -40 to 175 °C.

Figure 5(b) presents the optimized active inductor mean value, continuous line, and three standard deviation, in error bars. The results have a maximum variation of 139 ppm/°C for the  $L_t$ . Besides, a 1035 ppm/°C for  $R_t$  is found fluctuating around 400  $\Omega$  (figure not presented). A controlled and a small  $L_t$  variation over temperature is first presented here, which enables the use of AIs in harsh environments applications as smart vehicles.

#### 5 CONCLUSION

AIs have an interesting trade-off when inductor reconfiguration is required. However, its use in hash environments is limited due the usual high sensitivity to temperature effects. This paper presented a new temperature-aware design methodology to deal with this issue. Based on the  $g_m/I_D$  and sensitivity analysis, temperature variation is minimized when a counterintuitive transistor bias (WI)

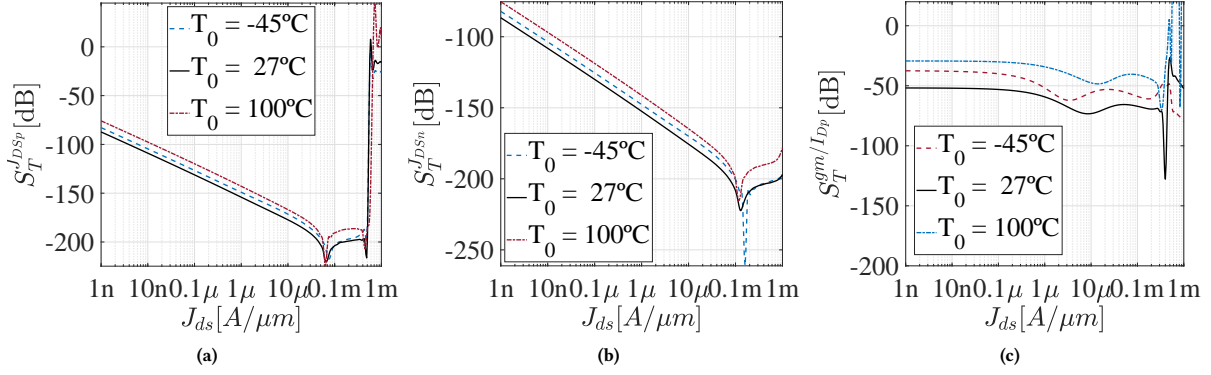


Figure 3: Ideal Wilson current mirror is used for parameters extraction: (a)  $S_T^{J_{DSp}}$  (b)  $S_T^{J_{DSn}}$  (c)  $S_T^{g_m/I_{Dp}}$

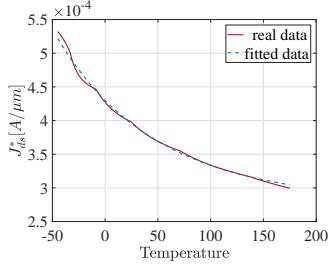


Figure 4: Sensitivity roots, and fitted data based on model presented in (17).

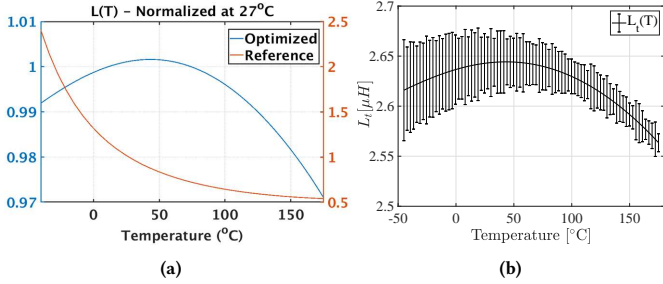


Figure 5: Post-layout Monte Carlo simulations from  $-40^{\circ}\text{C}$  to  $175^{\circ}\text{C}$ : (a) comparison between the optimized design in blue and reference design in orange; (b) variability analysis of the optimized design having the mean values in continuous line and  $3\sigma$  in error bars.

is used. An inductance variation as low as 139 ppm/ $^{\circ}\text{C}$  is reported

from  $-40$  to  $175^{\circ}\text{C}$ . The proposed methodology can be used to fabricate reliable low-power temperature-aware AIs suitable in harsh environments such as internet of things and autonomous cars applications.

## REFERENCES

- [1] Jawdat Abu-Taha and Metin Yazgi. 2016. A 7 GHz compact transimpedance amplifier TIA in CMOS  $0.18\ \mu\text{m}$  technology. *Analog Integrated Circuits and Signal Processing* 86, 3 (Mar 2016), 429–438.
- [2] Massimo Alioto. 2010. Understanding DC Behavior of Subthreshold CMOS Logic Through Closed-Form Analysis. *IEEE Trans. Circuits and Systems I: Regular Papers* 57, 7 (Jul 2010), 1597–1607.
- [3] B. Calvo et al. 2013. 1 V CMOS current references for wide-temperature range applications. *Electronics Letters* 49, 17 (Aug 2013), 1061–1063.
- [4] D. De Dorigo et al. 2015. Q-enhancement of a low-power gm-C bandpass filter for closed-loop sensor readout applications. In *IEEE Proc. of Int. Symp. Circuits Syst.* IEEE, Lisbon, Portugal, 678–681.
- [5] A. V. Fonseca et al. 2017. A Temperature-Aware Analysis of Latched Comparators for Smart Vehicle Applications. In *Proc ACM IEEE Symp. Integr. Circuits Syst. Design*. ACM, Fortaleza, CE, Brazil, 1–6.
- [6] C. Galup and M. Schneider. 2018. The compact all-region MOSFET model: theory and applications. In *IEEE New Circuits Syst. Conf.* IEEE, Montreal, QC, Canada, 166–169.
- [7] D. H. Jacobson. 1971. A general sufficiency theorem for the second variation. *J. Math. Anal. Appl.* 34, 3 (1971), 578–589.
- [8] V. Kumar and A. Islam. 2017. Study of variability performance of CMOS active inductors. *Microsyst. Technol.* (Dec 2017), 1–11.
- [9] W. Liu et al. 1998. *BSIM 3v3.2 MOSFET Model Users' Manual*. Technical Report. EECS Department, University of California, Berkeley.
- [10] J. Ou and P. M. Ferreira. 2018. Design considerations of CMOS active inductor for low power applications. *Analog Integr. Circ. Sig. Process* 94, 3 (Mar 2018), 347–356.
- [11] A. Saberkari et al. 2016. Active inductor-based tunable impedance matching network for RF power amplifier application. *Integration, the VLSI Journal* 52, 3 (Aug 2016), 301–308.
- [12] F. Silveira et al. 2016. A gm/Id Based Methodology for the Design of CMOS Analog Circuits and Its Application to the Synthesis of a Silicon-on-Insulator Micropower OTA. *IEEE J. Solid-State Circuits* 31, 9 (Sep 1996), 1314–1319.
- [13] S. M. Sze. 1981. *Physics of Semiconductor Devices* (2nd ed.). Jonh Wiley 'Sons, New York. 868 pages.
- [14] XFAB Mixed-Signal Foundry Experts. 2017. XH018 - 0.18 Micron Modular Analog Mixed HV Technology. . 22 pages.
- [15] F. Yuan. 2008. *CMOS Active Inductors and Transformers* (1st ed.). Springer, Boston, MA, USA. 290 pages.